Sciencexpress Reports

The COMPASS Subunit Spp1 Links Histone Methylation to Initiation of Meiotic Recombination

Laurent Acquaviva,[1]* Lóránt Székvölgyi,[2,4]* Bernhard Dichtl,[3]† Beatriz Solange Dichtl,[3] Christophe de La Roche Saint André,[1]† Alain Nicolas,[2]† Vincent Géli[1]†

[1]Marseille Cancer Research Center (CRCM), U1068 Inserm, UMR7258 CNRS, Aix-Marseille University, Institut Paoli-Calmettes, Marseille 13009, France. [2]Institut Curie Centre de Recherche, UMR3244 CNRS, Université Pierre et Marie Curie, 75248 Paris, France. [3]Centre for Cellular and Molecular Biology, School of Life & Environmental Sciences, Deakin University, Victoria, 3125 Australia. [4]Department of Biophysics and Cell Biology, Medical and Health Science Center, University of Debrecen, Hungary.

*These authors contributed equally to this work.

†To whom correspondence should be addressed. E-mail: b.dichtl@deakin.edu.au (B.D.); laroche@ifr88.cnrs-mrs.fr (C.d.L.R.S.A.); alain.nicolas@curie.fr (A.N.); geli@ifr88.cnrs-mrs.fr (V.G.)

Novel combinatorial associations of genetic traits arise from homologous recombination between parental chromosomes during meiosis. Histone H3 lysine 4 trimethylation marks meiotic recombination hotspots in yeast and mammals, but how this ubiquitous chromatin modification relates to initiation of Spo11-dependent double-strand breaks (DSB) remains unknown. Here we show that the tethering of the PHD-containing protein, Spp1, a component of the COMPASS complex to recombinationally cold regions is sufficient to induce DSB formation. Furthermore, we found that Spp1 physically interacts with Mer2, a key protein of the differentiated chromosomal axis required for DSB formation. Thus Spp1, by interacting with H3K4me3 and Mer2, promotes recruitment of potential meiotic DSB sites to the chromosomal axis, allowing Spo11 cleavage at nearby nucleosome-depleted regions.

Meiotic recombination is initiated by the introduction of DNA double-strand breaks (DSBs) by Spo11, a meiosis-specific transesterase, which is highly conserved throughout evolution (*1*). To ensure at least one crossover per chromosome pair, a large number of DSBs are formed in each meiotic cell, and their occurrence controlled at multiple levels comprising both higher-order chromosome structure and local determinants (*2*). In *S. cerevisiae*, approximately 150 DSBs are formed per meiosis, preferentially in promoter regions and with a highly variable frequency. DSBs sites are largely independent of DNA sequence composition (*3*). The control of DSB formation also depends on a number of Spo11-accessory proteins shown to form sub-complexes, but whose functions are only partially understood (*4*). In particular, the Mer2/Mei4/Rec114 complex plays a role in linking replication to subsequent DSB formation through Mer2 phosphorylation (*5*–*7*). This complex is also thought to tether potential DSB sites located on chromatin loops to the highly differentiated meiotic chromosome axis, leading to stepwise activation of Spo11 cleavage (*8*–*10*).

In *S. cerevisiae*, all H3K4 methylation is carried out by the COMPASS complex that includes Set1, the catalytic subunit, which acts as a scaffold for the other structural and regulatory components (*11*). In particular, the PHD-finger subunit Spp1 specifically regulates the H3K4me3 state (*11*, *12*). Our previous studies revealed that the absence of Set1 severely reduces meiotic DSB levels (*13*, *14*) and that the level of H3K4me3 is constitutively higher near DSB sites (*14*). However, beyond these correlations, the mechanistic link between H3K4 methylation and DSB formation remained to be elucidated (*15*).

To uncover functional connections, we first asked whether mutation of each COMPASS subunit affected DSB frequencies at natural recombination hot spots (*16*). Similar to deletion of *set1*, the absence of each COMPASS subunit, except Shg1, reduced DSB frequencies at the *BUD23* (Fig. 1A) and *CYS3* hotspots (fig. S1A; strain genotypes in table S1). Reduction was seen for Spp1, which is specifically required for H3K4me3 formation. The similar effect of *set1Δ* and *spp1Δ* mutants on DSB formation at hot spots also extends to DSB formation near the naturally cold *PES4* locus (fig. S1B) (*14*). To check if the decrease in DSB formation at hotspots only reflected the role of the COMPASS on H3K4 methylation, we asked whether it was recapitulated by mutation of the H3K4 residue. At *BUD23*, we observed equivalent DSB reduction in the *set1Δ* and *H3K4R* strains (fig. S1C). Parallel analysis of the *set1*Δ *H3K4R* double mutant revealed an identical effect, underscoring their epistatic relationship (fig. S1C). Altogether, these observations strongly support a role for the COMPASS complex and H3K4 tri-methylation in the control of DSB formation, and tie them to the same pathway.

Next, to elucidate the role of H3K4me3, Set1, and Spp1 in DSB formation, we asked whether the tethering of Set1 and Spp1 proteins to UAS_{GAL} binding sites located in cold DSB regions was sufficient to stimulate DSB formation, as previously observed for the GBD-Spo11 fusion (*17*). We generated and expressed in-frame fusions of the coding region with the Gal4 binding domain (GBD). With respect to H3K4 methylation and DSB formation, both GBD-Set1 and GBD-Spp1 fusions behaved the same as wild type, indicating no adverse interference with COMPASS and the Spo11 machinery (fig. S2 and table S2). We examined DSB formation in the naturally cold *GAL2* locus, which contains 5 UAS_{GAL} sequences in its promoter. Remarkably, the GBD-Set1 construct stimulated DSBs near the UAS_{GAL2} sites (fig. S3, A and B). In terms of genetic requirements, the data reported in fig. S3, C to E, establish that the GBD-Set1 induced DSBs were not associated with a coincident increase in H3K4me3 at *GAL2* but did depend on (i) the presence of Spo11, (ii) the integrity of the COMPASS, (iii) the histone methyl transferase activity of Set1, and (iv) the presence of the H3 lysine 4 residue.

Similar analyses revealed that GBD-Spp1 strongly stimulated DSB formation at *GAL2*. These DSBs appeared and disappeared upon repair with similar kinetics as natural DSBs (Fig. 1, B and C, see also Fig. 2A). Remarkably, DSBs targeted by GBD-Spp1 required neither the presence of Set1 or Bre2 nor the E3 ligase Bre1 that controls H3K4 trimethylation through the ubiquitinylation of H2B (*18*). In agreement with this observation, DSBs resulting from the tethering of Spp1 also appeared in the *H3K4R* mutant (Fig. 1D). Tethering Spp1 to the *GAL1*/*GAL10* and *GAL7* loci also efficiently induced DSBs (Fig. 2A), but surprisingly these breaks did not occur at the same location as those observed in the *GBD-SPO11* (Fig. 2B). While tethering of Spo11 introduced DSBs in the vicinity the *UAS* sites, tethering of Spp1 to the same sites produced cleavage in the 3′ end of the *GAL10* coding sequence (Fig. 2B and fig. S4A). As for the majority of meiotic DSBs in *S. cerevisiae* which occurs

in promoter regions, the unexpected location of these GBD-Spp1 induced DSBs coincides with the promoter of the well-characterized antisense *GAL1* ucut (SUT013) non-coding RNA. This RNA is expressed in meiosis (*19*) under the control of the transcription factor Reb1 (*20*). This situation is also consistent with the high-resolution genome wide map of DSBs, which revealed a high enrichment of Spo11 binding in nucleosome-depleted regions adjacent to the Reb1 binding sites (*3*). As in *GAL2*, the DSBs generated at *GAL10* required Spo11 and occurred in the absence of H3K4 methylation (fig. S4B). Altogether, these results demonstrated that the tethering of Spp1 efficiently stimulated Spo11-dependent DSBs independently of H3K4 methylation.

A simple interpretation of the above results is that Spp1 recruits a component of the DSB machinery. To search for interaction partners, we performed yeast two-hybrid screening using the full length Spp1 protein (*16*). We readily identified Set1 and Mer2 as prominent interactors of Spp1 (table S3). The Spp1-interacting region of Mer2 was mapped to the central part of the protein (residues 105 to 172) (fig. S5A). The Mer2-Spp1 interaction was validated by GST-Mer2 pull-down experiments using various in vitro translated Spp1 polypeptides. We found that the 131 aa C-terminal region of Spp1 was required for interaction with Mer2 (fig. S5B). Finally, we examined the in vivo interaction of Spp1 and Mer2 during meiosis using tagged versions of both proteins. The C-terminally tagged *SPP1-HA3* strain showed nearly wild type level of H3K4me3 and a slight reduction (35%) of DSB formation at the *BUD23* hotspot but nevertheless wild-type spore viability, indicating efficient DSB formation genome-wide (fig. S6 and table S2). Spp1-HA3 was efficiently co-immunoprecipitated with Mer2-myc9 during meiosis, with a peak at 4 hours (Fig. 3A). DNase and phosphatase treatments of the Myc immunoprecipitated proteins from the double-tag strain did not reduce the recovery of Spp1-HA (fig. S5, B and C), suggesting an interaction of Spp1 with the non-phosphorylated form of Mer2 (*5*, *7*, *9*). A schematic representation of the Spp1-Set1 and Spp1-Mer2 interaction domains is illustrated in fig. S5D.

The essential role of Mer2 in DSB formation and its interaction with Spp1 prompted us to determine whether Mer2 was present at the Spp1-tethered DSB sites. At the control *CTR86* and *SED4* regions known to associate with Mer2 in wild-type cells (*9*), we found that Mer2 was enriched in the strains expressing GBD and GBD-Spp1 (fig. S7A), suggesting that the expression of these GBD fusion proteins did not alter chromatin occupancy of Mer2. Four hours after transfer to the SPM sporulation media, Mer2 was strongly enriched at the UAS_{GAL} sites in the strain expressing GBD-Spp1, but not in the strains expressing *GBD* alone (Fig. 3B). Importantly, Mer2-myc was also enriched in the vicinity of the Gal1 ucut promoter where the major DSB site is detected (Fig. 3C). This enrichment appears to be specific as its level is greater than the one expected to spread for the UAS sites.

Examination of the genetic requirements for DSB formation indicated that the cleavage site induced by the tethering of Spp1 was (i) independent of Set1, (ii) required Mer2, and (iii) did not result from Spp1 overexpression (fig. S7B). The previously described Spp1 zinc finger-like domain (SZF) was included in the Mer2-interacting region (*21*). We deleted the SZF canonical CXXC motif in GBD-Spp1 (GBD-$Spp1_{\Delta CXXC}$) and tested whether deleting this evolutionary conserved motif impairs DSB formation and Mer2 binding at *GAL10* (*16*). DSB formation and Mer2 binding were both strongly reduced at *GAL10* providing a strong correlation between the ability of GBD-Spp1 to recruit Mer2 at *GAL10* and DSB formation (fig. S8). This outlines the importance of this interaction for DSB formation.

What is the role of H3K4 methylation in the control of DSB formation? We found that the amount of Spp1 was strongly reduced both in the absence of Set1 and in COMPASS mutants affecting the stability of Set1, but either remained normal in the catalytically inactive *set1G951S* mutant or was slightly reduced in the *H3K4R*, *bre2*Δ and *sdc1*Δ mutants (fig. S9, A and B). Therefore, decreased levels of Spp1 might only partially explain the DSB formation defect of mutants that are compromised in H3K4 methylation. Our interpretation is that the function of Spp1 in DSB formation depends on H3K4 methylation through an interaction of its PHD-finger with H3K4me2/3 (*21*). We therefore deleted the PHD domain of Spp1 (*16*) and tested whether the presence of the PHD domain was important for H3K4me3 and DSB formation. We detected nearly wild-type level of H3K4me3 in the $spp1_{\Delta PHD}$ mutant (Fig. 4A), whereas DSB formation was clearly reduced at the *BUD23* and *CYS3* hotspots (Fig. 4B). We conclude that the Spp1 PHD domain itself plays a specific role in DSB formation.

Our work led us to propose an enriched chromatin loop-axis model (Fig. 4C) for the regulation of DSB formation that addresses how the meiotic DSB sites are mechanistically selected. We propose that the interaction between the COMPASS subunit, Spp1, and Mer2 brings potential meiotic DSB sites to the chromosome axis for further downstream events that will ultimately lead to Spo11-dependent DSB formation at axis-proximal regions that are depleted of nucleosomes. In mammals, H3K4 methylation has been reported to be enriched at recombination hotspots where the meiosis specific PRDM9 H3K4 methyltransferase is known to act (*22*–*24*). How PRDM9 connects to the mammalian DSB machinery is not known but as in yeast, it may be the consequence of a direct interaction with a protein of the DSB machinery. Our results indicate that H3K4me3 is required for the function of Spp1, probably through its recognition by the PHD-domain within Spp1, and this requirement can be bypassed by tethering Spp1 to the DNA locus. The broadly localized H3K4me3 modification has the virtue of permitting the initiation of recombination at numerous places of the genome, a molecular strategy that ensures a large diversity of recombinant haplotypes to be transmitted by the gametes. In conclusion, this model offers a clue of how chromosome structure and DSB regulation are interrelated, and it attributes a pivotal role to Spp1 in the recruitment of components acting at meiotic DSB sites to the chromosomal axis.

References and Notes

1. D. Zickler, N. Kleckner, Meiotic chromosomes: Integrating structure and function. *Annu. Rev. Genet.* **33**, 603 (1999). doi:10.1146/annurev.genet.33.1.603 Medline
2. M. Lichten, B. de Massy, The impressionistic landscape of meiotic recombination. *Cell* **147**, 267 (2011). doi:10.1016/j.cell.2011.09.038 Medline
3. J. Pan *et al.*, A hierarchical combination of factors shapes the genome-wide topography of yeast meiotic recombination initiation. *Cell* **144**, 719 (2011). doi:10.1016/j.cell.2011.02.009 Medline
4. S. Keeney, Spo11 and the formation of DNA double-strand breaks in meiosis. *Genome Dyn Stab.* **2**, 81 (2008). doi:10.1007/7050_2007_026 Medline
5. K. A. Henderson, K. Kee, S. Maleki, P. A. Santini, S. Keeney, Cyclin-dependent kinase directly regulates initiation of meiotic recombination. *Cell* **125**, 1321 (2006). doi:10.1016/j.cell.2006.04.039 Medline
6. J. Li, G. W. Hooker, G. S. Roeder, *Saccharomyces cerevisiae* Mer2, Mei4 and Rec114 form a complex required for meiotic double-strand break formation. *Genetics* **173**, 1969 (2006). doi:10.1534/genetics.106.058768 Medline
7. H. Sasanuma *et al.*, Cdc7-dependent phosphorylation of Mer2 facilitates initiation of yeast meiotic recombination. *Genes Dev.* **22**, 398 (2008). doi:10.1101/gad.1626608 Medline
8. Y. Blat, R. U. Protacio, N. Hunter, N. Kleckner, Physical and functional interactions among basic chromosome organizational features govern early steps of meiotic chiasma formation. *Cell* **111**, 791 (2002). doi:10.1016/S0092-8674(02)01167-4 Medline
9. S. Panizza *et al.*, Spo11-accessory proteins link double-strand break sites to the chromosome axis in early meiotic recombination. *Cell* **146**, 372 (2011). doi:10.1016/j.cell.2011.07.003 Medline
10. T. Miyoshi *et al.*, A central coupler for recombination initiation linking chromosome architecture to S phase checkpoint. *Mol. Cell* **47**, 722 (2012). doi:10.1016/j.molcel.2012.06.023 Medline

11. P. M. Dehé *et al*., Protein interactions within the Set1 complex and their roles in the regulation of histone 3 lysine 4 methylation. *J. Biol. Chem.* **281**, 35404 (2006). doi:10.1074/jbc.M603099200 Medline
12. J. Schneider *et al*., Molecular regulation of histone H3 trimethylation by COMPASS and the regulation of gene expression. *Mol. Cell* **19**, 849 (2005). doi:10.1016/j.molcel.2005.07.024 Medline
13. J. Sollier *et al*., Set1 is required for meiotic S-phase onset, double-strand break formation and middle gene expression. *EMBO J.* **23**, 1957 (2004). doi:10.1038/sj.emboj.7600204 Medline
14. V. Borde *et al*., Histone H3 lysine 4 trimethylation marks meiotic recombination initiation sites. *EMBO J.* **28**, 99 (2009). doi:10.1038/emboj.2008.257 Medline
15. S. E. Tischfield, S. Keeney, Scale matters: the spatial correlation of yeast meiotic DNA breaks with histone H3 trimethylation is driven largely by independent colocalization at promoters. *Cell Cycle* **11**, 1496 (2012). doi:10.4161/cc.19733 Medline
16. Materiels and methods are available as supplementary materials on *Science* Online.
17. A. Peciña *et al*., Targeted stimulation of meiotic recombination. *Cell* **111**, 173 (2002). doi:10.1016/S0092-8674(02)01002-4 Medline
18. A. Wood *et al*., Bre1, an E3 ubiquitin ligase required for recruitment and substrate selection of Rad6 at a promoter. *Mol. Cell* **11**, 267 (2003). doi:10.1016/S1097-2765(02)00802-X Medline
19. A. Lardenois *et al*., Execution of the meiotic noncoding RNA expression program and the onset of gametogenesis in yeast require the conserved exosome subunit Rrp6. *Proc. Natl. Acad. Sci. U.S.A.* **108**, 1058 (2011). doi:10.1073/pnas.1016459108 Medline
20. M. Pinskaya, A. Nair, D. Clynes, A. Morillon, J. Mellor, Nucleosome remodeling and transcriptional repression are distinct functions of Isw1 in *Saccharomyces cerevisiae*. *Mol. Cell. Biol.* **29**, 2419 (2009). doi:10.1128/MCB.01050-08 Medline
21. B. L. Murton, W. L. Chin, C. P. Ponting, L. S. Itzhaki, Characterising the binding specificities of the subunits associated with the KMT2/Set1 histone lysine methyltransferase. *J. Mol. Biol.* **398**, 481 (2010). doi:10.1016/j.jmb.2010.03.036 Medline
22. F. Baudat *et al*., PRDM9 is a major determinant of meiotic recombination hotspots in humans and mice. *Science* **327**, 836 (2010). doi:10.1126/science.1183439 Medline
23. S. Myers *et al*., Drive against hotspot motifs in primates implicates the *PRDM9* gene in meiotic recombination. *Science* **327**, 876 (2010). doi:10.1126/science.1182363 Medline
24. F. Smagulova *et al*., Genome-wide analysis reveals novel molecular features of mouse recombination hotspots. *Nature* **472**, 375 (2011). doi:10.1038/nature09869 Medline
25. H. Murakami, A. Nicolas, Locally, meiotic double-strand breaks targeted by Gal4BD-Spo11 occur at discrete sites with a sequence preference. *Mol. Cell. Biol.* **29**, 3500 (2009). doi:10.1128/MCB.00088-09 Medline
26. C. Fairhead, B. Llorente, F. Denis, M. Soler, B. Dujon, New vectors for combinatorial deletions in yeast chromosomes and for gap-repair cloning using "split-marker" recombination. *Yeast* **12**, 1439 (1996). doi:10.1002/(SICI)1097-0061(199611)12:14<1439::AID-YEA37>3.0.CO;2-O Medline
27. N. Robine *et al*., Genome-wide redistribution of meiotic double-strand breaks in *Saccharomyces cerevisiae*. *Mol. Cell. Biol.* **27**, 1868 (2007). doi:10.1128/MCB.02063-06 Medline
28. P. Luciano *et al*., RPA facilitates telomerase activity at chromosome ends in budding and fission yeasts. *EMBO J.* **31**, 2034 (2012). doi:10.1038/emboj.2012.40 Medline
29. L. Zhang, H. Ma, B. F. Pugh, Stable and dynamic nucleosome states during a meiotic developmental process. *Genome Res.* **21**, 875 (2011). doi:10.1101/gr.117465.110 Medline
30. A. Halbach *et al*., Cotranslational assembly of the yeast SET1C histone methyltransferase complex. *EMBO J.* **28**, 2959 (2009). doi:10.1038/emboj.2009.240 Medline
31. D. P. Mersman, H. N. Du, I. M. Fingerman, P. F. South, S. D. Briggs, Charge-based interaction conserved within histone H3 lysine 4 (H3K4) methyltransferase complexes is needed for protein stability, histone methylation, and gene expression. *J. Biol. Chem.* **287**, 2652 (2012). doi:10.1074/jbc.M111.280867 Medline

Acknowledgments: We thank F. Klein and V. Borde for materials and S. Kowalczykowski for reading of the manuscript. Work in the V.G. and A.N. laboratories is supported by the "Ligue contre le Cancer" (Equipe Labelisées). Work in the laboratory of B.D. was supported by the Swiss National Science Foundation. L.A. was supported by grants from the Fondation ARC and L.S. by the European Union and the Hungarian Research Fund.

Supplementary Materials

www.sciencemag.org/cgi/content/full/science.1225739/DC1
Materials and Methods
Figs. S1 to S9
Tables S1 to S5
References (*26–31*)

6 June 2012; accepted 5 November 2012
Published online 15 November 2012
10.1126/science.1225739

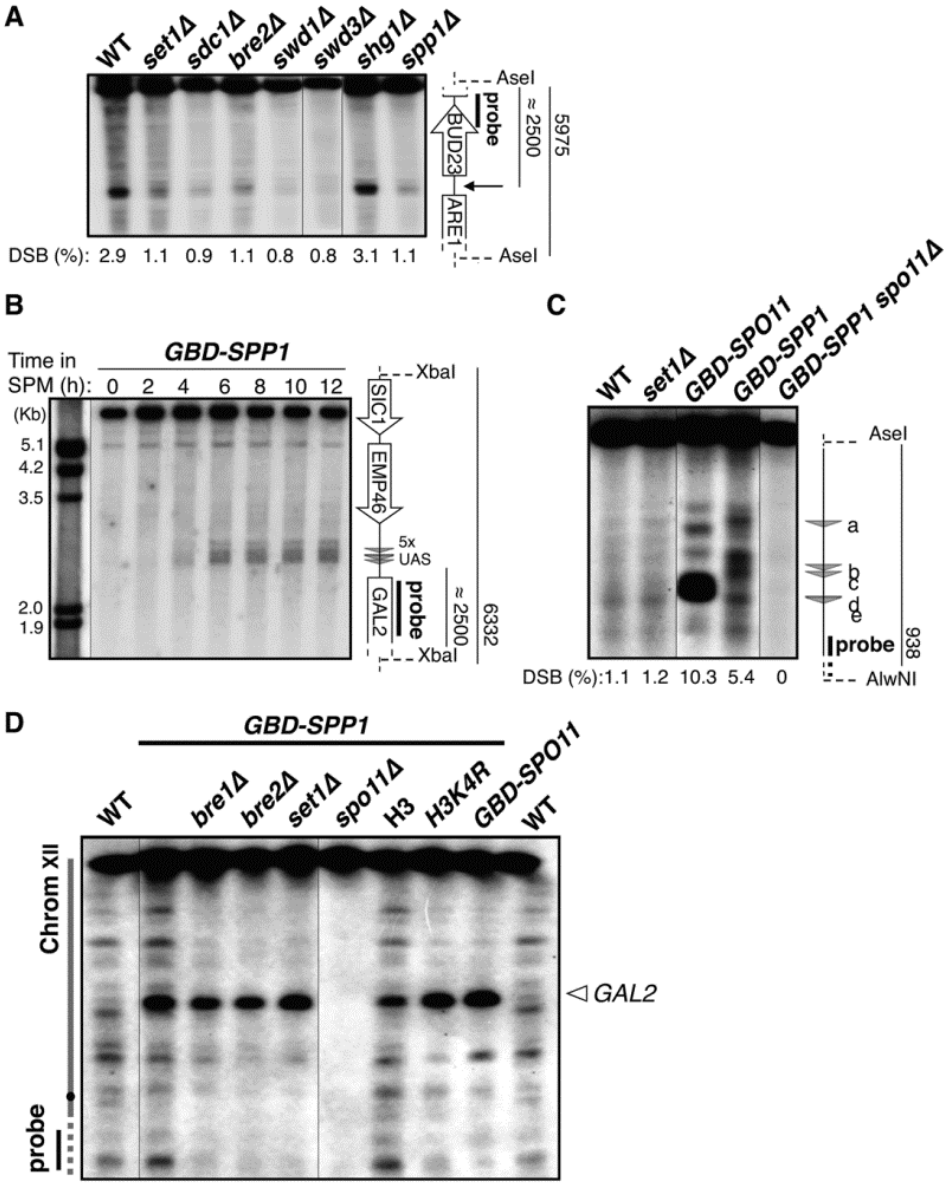

Fig. 1. GBD-Spp1 induces H3K4me3-independent meiotic DSBs at *GAL2*. (**A**) DSB formation in COMPASS mutants was analyzed by Southern blot at the *BUD23-ARE1* region. The arrow indicates the DSB site. Quantification of the prominent DSB fragments (% of DSB fragment/total DNA) is indicated below the gel. (**B**) DSB analysis at *GAL2* of *GBD-SPP1* cells harvested at different times after transfer into SPM. (**C**) High resolution analysis of DSBs at *GAL2* 16 hours after transfer to SPM was performed as described in (*25*). The 5 UAS_{GAL2} are indicated by gray triangles. (**D**) Southern blot analysis of DNA extracted from *GBD-SPP1* cells carrying the indicated mutations. Genomic DNAs were separated by PFGE and visualized with a chromosome XII left-end probe. *GBD-SPO11* and WT are used as controls.

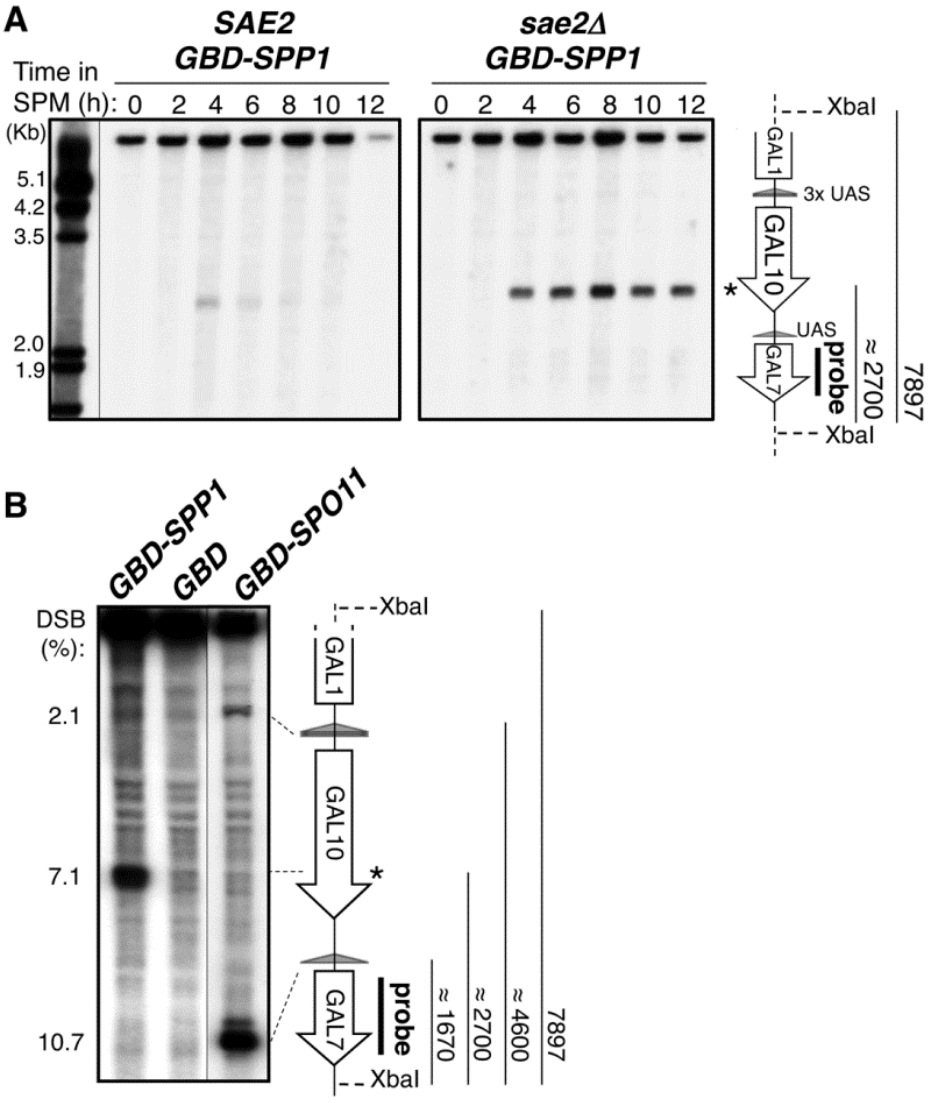

Fig. 2. GBD-Spp1 induces DSBs distal to the $UAS_{GAL7\text{-}GAL10}$. (**A**) Kinetics of DSB formation at *GAL10* induced by GBD-Spp1 in *SAE2* and *sae2*Δ cells. (**B**) Analysis of DSB formation in the *GAL1-GAL7* region (*GAL7* probe). The position of the DSBs induced by GBD-Spp1 is indicated by an asterisk.

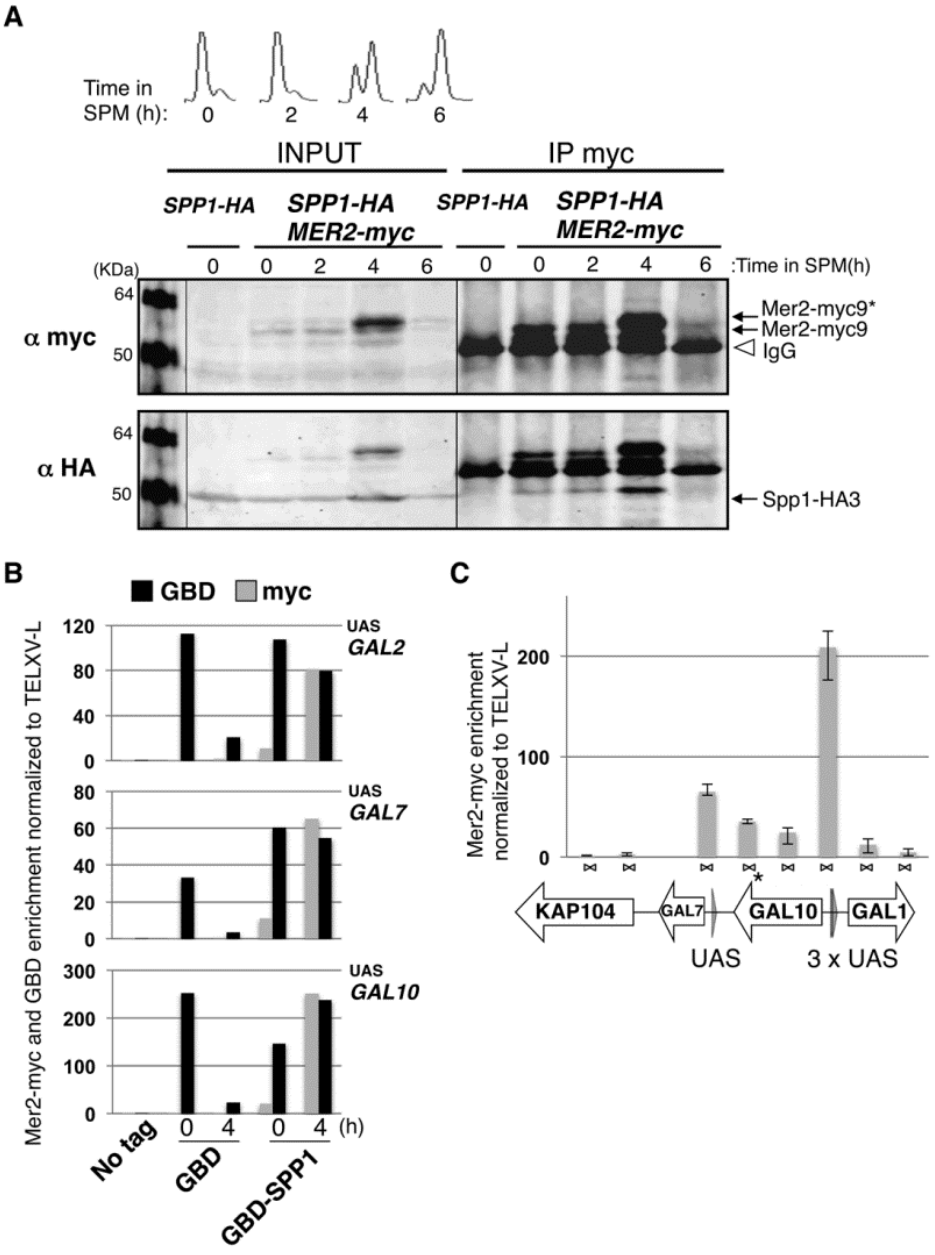

Fig. 3. Spp1 interacts with Mer2. (**A**) Top: DNA replication monitored by FACS. Bottom: protein extracts (INPUT) and myc-immunoprecipitated proteins (IP myc) from a Spp1-HA3 Mer2-myc9 strain were analyzed by Western blot with an anti-myc antibody (upper gel) and reprobed with an anti-HA antibody (lower gel) (*16*). Arrows indicate the positions of Mer2-myc9 (asterisk: phosphorylated form) and Spp1-HA3. A strain expressing only Spp1-HA3 was used as negative control. (**B**) *GBD*, *GBD-SET1*, and *GBD-SPP1* strains expressing Mer2-myc9 were harvested after 0 and 4 hours in SPM. Binding of the GBD-fusion proteins and Mer2-myc9 at the *GAL2*, *GAL7*, and *GAL10* UASs was analyzed by ChIP with anti-GBD and anti-myc antibodies. PCR primers specific for each GAL_{UAS} and TELXV-L (control) were used to amplify immunoprecipitated DNAs (*16*). (**C**) Chromatin binding of Mer2-myc9 in the *GBD-SPP1* strain was analyzed by ChIP-qPCR after 4 hours in SPM along the genomic region comprising *GAL7*, *GAL10*, and *GAL1* at positions indicated by two convergent arrowheads. The asterisk indicates the Gal1 ucut promoter.

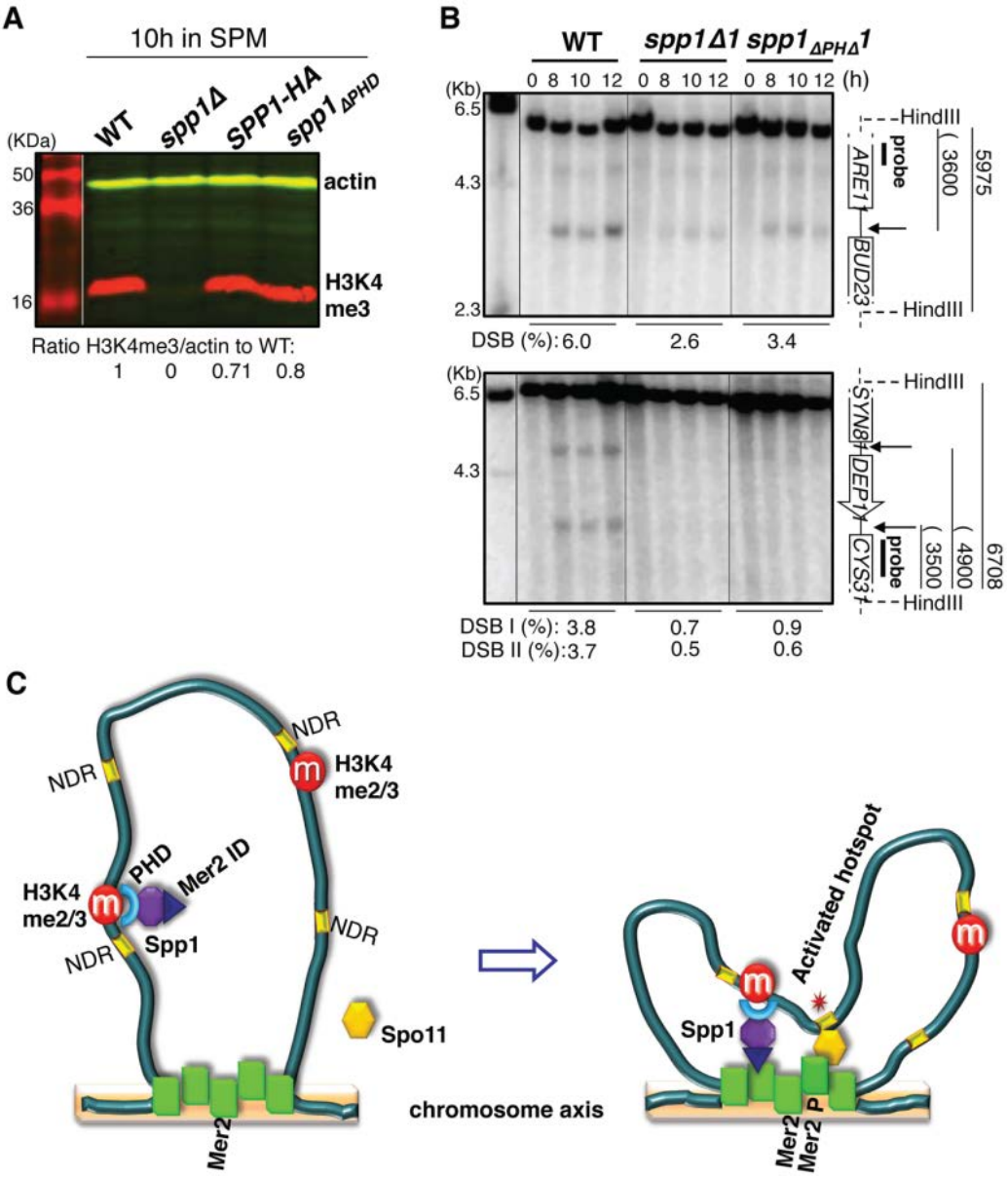

Fig. 4. The PHD-finger domain of Spp1 regulates meiotic DSB formation. (**A**) Analysis of H3K4me3 levels (*16*). (**B**) DSB formation at the *BUD23* and *CYS3* hotspots. (**C**) Extension of the chromatin loop-axis model. The tethering of a H3K4me-rich region to the chromosomal axis via the Spp1-Mer2 interaction allows Spo11 cleaveage at a proximal nucleosome-depleted region (NDR).

The COMPASS Subunit Spp1 Links Histone Methylation to Initiation of Meiotic Recombination

Laurent Acquaviva, Lóránt Székvölgyi, Bernhard Dichtl, Beatriz Solange Dichtl, Christophe de La Roche Saint André, Alain Nicolas and Vincent Géli (November 15, 2012)

published online November 15, 2012

Editor's Summary